

## Experimental Study on Deformation and Destruction of Post-peak Fractured Rock Mass

Luchen ZHANG\*, Shuchen LI, Yang PING

Geotechnical and Structural Engineering Research Center, Shandong University,

Jinan jingshi road No.17923, Shandong,250061, China

zhangchen411@163.com

271539204@qq.com

**Keywords:** different confining pressure; fractured rock mass; triaxial test; Post-peak

**Abstract.** The stress-strain curve of fractured rock mass can be divided into two parts, the pro-peak and post-peak. The pro-peak part of the rock stress-strain curve is generally stable and its mechanical behavior can be described with classical strength theory. Rock post-peak stress is very complex and generally is in unstable state, its mechanical behavior is hard to be described with classical strength theory. In this paper, the cylinder standard specimens with different angle of pre-existing transfixion joint are carried through conventional triaxial compression test under different confining pressure, in order to analyze deformation and destruction of fractured rock mass. The results show that the post-peak of fractured rock mass stress-strain curve changes unstable and very complex; Yield strength, peak intensity and residual strength of the rock specimens proportional to the change in confining pressure. Under the condition of low confining pressure, stress-strain relationship of fractured rock mass conform to the ideal elastic brittle model; under high confining pressure, its relations conform to the ideal elastic-plastic model. Within a certain range, relative to the confining pressure, the joint angle has greater impact on the damage type of fractured rock mass.

### Introduction

Mechanical behavior of post-peak fractured rock mass is always important and difficult points in the field of rock mechanics research. The bearing capacity of the rock bursts when the peak strength is achieved, broken rock mass generates significant dilatancy effect in post-peak area. The research on characteristics of deformation and failure of rock material mechanical behavior delivers important significance for guiding roadway support [1].

Paulding, Hoek and Bieniawski, et al[2,3,4,5]early explored the stress-strain curve in the whole process of rock. Yang Z Y, et al[6] conducted uniaxial compression test on the through joint rock, pointed out that the destruction form of through joint rock mass was splitting, slipping along the joint surface and combined failure of splitting and slip, analyzed major reasons causing different failure modes, strengths and deformations of specimen. Sun Guangzhong raised the control theory of rock mass structures[7,8], and proposed that the rock mass structure controlled the deformation and failure of rock mass and its mechanical properties. Sun jun conducted the unloading test by the method of inserting sheet steel and pulling out slight tension fractures with cement mortar specimens, and the compared and analyzed the feature deformation and strength characteristics of rock mass under conditions of loading and unloading [9,10].

The abovementioned scholars mainly concentrate research on changes in pre-peak rock mass destruction features, rare literatures focus on post-peak deformation characteristics. Conventional triaxial compression testes are conducted on throughout & fractured rock masses in this paper, through different confining pressures and angles of inclination, and post-peak deformation and failure process of fractured rock masses are analyzed. Research results can truly reflect deformation characteristics of surrounding rocks of underground works, providing certain basis for supporting design and construction of surrounding rock.

## Triaxial Compression Test

Standard cylindrical rock blocks including throughout joints with the height of 100mm and the diameter at 50mm are selected as specimens for this tests, ( $q$  stands for the included angle between the loading surface and the joint surface),  $q$  is respectively valued  $0^\circ$ ,  $20^\circ$ ,  $40^\circ$  and  $60^\circ$  in tests. The confining pressures adopted involve 3 MPa, 5 MPa, 7 MPa and 9 MPa.

The specimen using 425 # ordinary Portland cement, sand, water and early-strength water-reducing agent matched in certain proportion ratio, the stalloy with the thickness at 0.1 mm is inserted along the chiseled groove of the mold, prefabricating out throughout joints with different inclination. The core is taken out by aligning to the block after curing to develop into standard cylinder block as shown in Figure 1. Figure 2 is the figure for RLW-1000 type servo triaxial press and displacement sensor device.



Fig.1 Schemes of jointed specimen Fig.2 RLW-1000 servo-controlling testing machine

## Analysis on test results

The full process of stress and strain in the whole course of test is automatically acquired and recorded computer, each sandstone specimen containing throughout joint angle is subjected to repeated testes with exactly identical test conditions, the medians are selected to represent test results.

Stress-strain relationship of fractured rock masses under different confining pressures

Under the condition of constant fracture dip angle, the stress and strain curves of different confining pressures are shown in Figure 3.

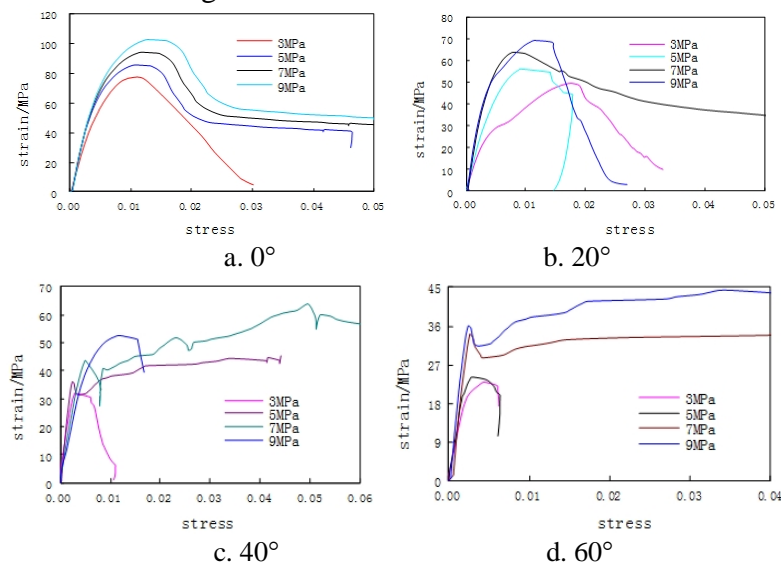


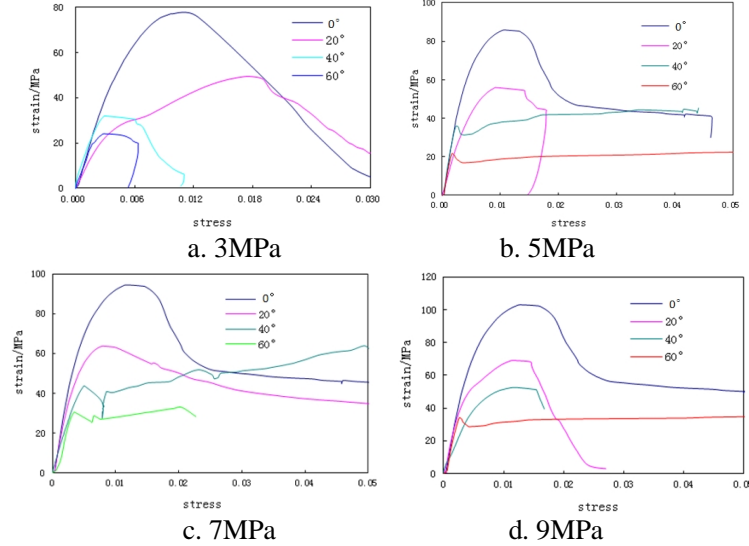
Fig.3 Fractured rock mass stress-strain curve under different confining pressures

Figure 3 shows that the yield strength, peak intensity and residual strength of fractured rock mass specimen basically increases with the increase in the confining pressure, when the confining pressure hits 3MPa, 5MPa, 7MPa and 9MPa respectively, and the stress-strain curve enters into the softening stage after the peak point, the stress decreases to residual strength with the increase in the strain. Fractured rock mass falls after the peak value under the condition of low confining pressure, being characterized by strain softening, and the stress-strain relation of fractured rock mass conforms to ideal

elastic brittle model. The change in post-peak stress is insignificant under high confining pressure, and the stress-strain relation of fractured rock mass conforms to ideal elastic-plastic model.

#### Stress-strain relationship of fractured rock mass under different inclination

The stress-strain relations of fractured rock masses under the confining pressure at 3MPa, 5MPa, 7MPa and 9MPa and the dip angle at 0°, 20°, 40° and 60° are shown in Figure 4.



**Fig.4. Stress-strain relationship curve of fractured rock under different inclination**

In Figure 4, the change forms of pre-peak stress-strain curves of fractured rock mass are similar when the confining pressure is constant, and the tendency of post-peak stress-strain curve differs, the peak strength of complete specimen is the greatest, and the peak strength decreases in the increase in the dip angle. Its peak strength is one third of that of complete specimen when the dip angle hits 60°; The smaller of change in plastic deformation will be when greater dip angle of joint is, suggesting that both the peak strength and residual strength of specimen are sensitive to the confining pressure, and such rock specimen is classified to be brittle plastic. The peak strain value of throughout fractured rock mass decreases with the increase in the dip angle of fracture, and it increases accordingly within the increase in the confining pressure.

#### Failure Mode of Post-peak Fractured Rock Mass

It is assumed that maximum principal stress in fractured rock mass forms the joint at  $q$  with vertical surface into the joint. Normally the fractured rock mass generally generates two failure modes when it is stressed: Splitting failure of intact rock mass and failure along structural plane. It is assumed that the strength characteristics of intact rock and structural surface meet the strength theory of Moore-Coulomb straight line, then it can be concluded from Mohr-Coulomb criterion.

$$s_1 - s_3 = \frac{2s_3 \tan j_j + 2c_j}{(1 - \tan j_j \cot q) \sin 2q} \quad (1)$$

The rock specimen will suffer from the failure along structural surface when  $s_1 \geq s_3 + \frac{2s_3 \tan j_j + 2c_j}{(1 - \tan j_j \cot q) \sin 2q}$  is satisfied; The sliding along the structural surface won't occur when the abovementioned inequation is not satisfied, and it is only possible to generate the rupture irrelevant to the discontinuity surface, in this case the following conditions will be met when the rock specimen is failed:

$$s_1 \geq s_3 + s_3(N_f - 1) + 2c\sqrt{N_f} \quad (2)$$

In the equations  $N_f = \frac{1 + \sin j}{1 - \sin j}$ , where  $c$  and  $c_j$  respectively represents binding powers of rock and structural plane; while  $j$  and  $j_j$  respectively represent internal friction angles of rock and structural plane.

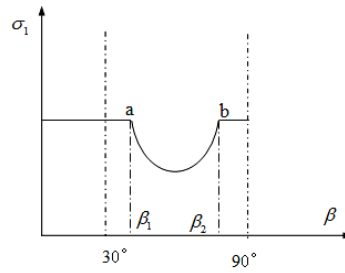


**Fig.5 The relationship curve of  $s_1$  and  $q$**

Maximum principal stress alters with the change in  $b$  when the surrounding rock  $s_3$  is constant, clearly showing anisotropy function of structural surface strength (shown in Figure 5). Point a and Point b in Figure 5 indicates the specimen of fractured rock mass is about to generate the failure along the structural surface and the splitting failure of intact rock, the structural surfaces  $b_1$  and  $b_2$  may be obtained according to geometrical relationship between the stress circle and the structural surface, and then

$$b_1 = \frac{p + j_j - \arcsin \left[ \left( \frac{s_m + c_j \cot j_j}{t_m} \right) \sin j_j \right]}{2} \quad (3)$$

$$b_2 = \frac{j_j + \arcsin \left[ \left( \frac{s_m + c_j \cot j_j}{t_m} \right) \sin j_j \right]}{2} \quad (4)$$

Where,  $s_m = \frac{s_1 + s_3}{2}$ ,  $t_m = \frac{s_1 - s_3}{2}$

It may be determined that the failure along the structural surface of the specimen will occur when the dip angle  $q$  of structural surface containing throughout fractured rock mass by combining abovementioned analysis, and the specimen is likely to undergo structural failure when  $q > b_1$  or  $q < b_2$  is satisfied.

The failure forms of different confining pressures are obtained by calculations on abovementioned equations. Triaxial test of intact specimen shows obvious split and failure characteristics. The failure mode roughly the same to that of intact block and the dip angle of 20°. The failure and sliding along the fracture surface will occur as shown in Figure 6 when the dip angle is 40° and 60°. The dip angle of fractured rock imposes a greater influence on the failure form of fractured mass rock within a certain range, when compared to that of the confining pressure.

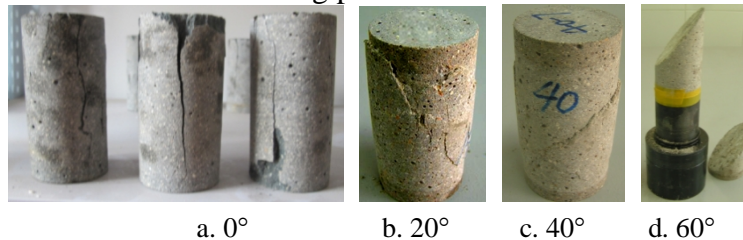


**Fig.6 Failure characteristics of fractured rock under different inclination**

## Conclusions

The throughout fractured rock mass specimens with different fracture dip angles are subjected to conventional triaxial compression tests, and post-peak failure characteristics of fractured rock mass deformation are analyzed. Research results can may truly reflect the deformation characteristics of

surrounding rocks in deep underground works under different confining pressures and fracture dip angles, providing a certain basis for supporting design for surrounding rocks.

(1) The shape of change in the pre-peak stress-strain curve of rock mass specimen is similar, and the tendency is consistent, but the change in post-peak stress-strain curve is instable or extremely complex. When the confining pressure is low, the fractured rock mass suffer from the stress drop after peak value, showing strain softening, and its stress-strain relation coincides with ideal elasticity plasticity and brittleness model; The stress-strain relation of fractured rock mass coincides with elasticity plasticity and brittleness model under high confining pressure.

(2) The yield strength, peak strength and residual strength of rock specimens basically increase linearly increases with the increase in the confining pressure. The peak intensity of fractured rock mass decreases with the increase in the dip angle of fracture when the confining pressure is constant, and the rock mass is characterized by brittle and plastic featured when the smaller the plastic deformation is. The influence of joint angle on the failure mode of fractured rock mass is greater relative to the confining pressure within certain range.

## References

- [1] Dong Fangting, Song Hongwei, GuoZhihong. Roadway support theory based on broken rock zone[J]. Journal of china coal society, 1994, 19(1): 21-32.
- [2] Paulding BW, Crack growth during brittle fracture in compression [D]:.PhD. thesis, MIT, Cambridge, MA, 1965.
- [3] Hoek E. Rock fracture under static stress conditions [R]. Pretoria, South Africa: National Mechanical Engineering Research Institute, CSIRO, 1965.
- [4] E. Hoek, M.S. Diederichs. Empirical estimation of rock mass modulus [J]. International Journal of Rock Mechanics & Mining Seienees, 2006, 43(2): 203-215.
- [5] Bieniawski ZT. Mechanism of brittle fracture of rock, Parts I , II and III [J]. Internation: Journal of Rock Mechanics and Mining sciences & Geomechanics Abstracts, 1967, 4(4): 395-430.
- [6] Yang ZY, Chen JM, Huang TH. Effect of joint sets on the strength and deformation of rock mass models[J]. International Journal of Rock Mechanics and Mining Science, 1998, 35(1): 75-84.
- [7] Sun Guangzhong. Rock mass structure mechanics[M]. Beijing: Science Press, 1988.
- [8] Sun Guangzhong. On the theory of structure-controlled rock mass[J]. Journal of engineering geology, 1993.9(First issue): 14-18.
- [9] Wu Gang. Comparison of failure effects of rock mass under loading and unloading conditions[J]. Rock and Soil Mechanics, 1997, 18(2): 13-16.
- [10] Wu Gang, Sun Jun. Deformation and strength characters of jointed rock mass under unloading stress states[J]. Chinese Journal of Rock Mechanics and Rock Engineering, 1998, 17(6): 615~621.